IEEE 1588 (PTP) over mmWave 5G NR: preliminary assessment of the synchronization accuracy for TSN applications

Alberto Morato*, Elena Ferrari§, Claudio Zunino*, Manuel Cheminod*, Stefano Vitturi*, and Federico Tramarin‡
*National Research Council of Italy, CNR-IEIIT
Email: {alberto.morato, claudio.zunino, manuel.cheminod, stefano.vitturi}@ieiit.cnr.it,
§ Dipartimento di Ingegneria dell'informazione, Università di Padova
Email: elena.ferrari.7@phd.unipd.it,
†Department of Engineering "Enzo Ferrari", University of Modena and Reggio Emilia, Modena, Italy
Email: federico.tramarin@unimore.it

***Abstract*—The extension of Time Sensitive Networking (TSN) to wireless domains is a key enabler for the realization of Industry 4.0 and 5.0 applications. Thanks to their characteristics in terms of latency and bandwidth, and the seamless integration with Ethernet TSN, 5G New Radio (NR) and 802.11 (WiFi) are the primary candidates for enabling wireless TSN applications. In the TSN context, precise time synchronization represents a fundamental building block. In this paper, we focus on the assessment of the synchronization accuracy of IEEE 1588 (PTP) over 5G NR networks by considering different network configurations and traffic loads. The results provide preliminary insights into the performance of PTP over 5G NR and its suitability for TSN applications.**

***Index Terms*—5G New Radio (NR), Precision Time Protocol (PTP), Time Sensitive Networking (TSN), Wireless time synchronization, Network Quality of Service (QoS), Hybrid TSN architectures**

I. Introduction

Among the available wireless technologies, 5G and 802.11, are the primary candidates for enabling wireless Time Sensitive Networking (TSN) applications. Both technologies are potentially able to provide the Quality of Service (QoS), latency and bandwidth requirements to enable realtime distributed industrial and measurement applications [1]–[3]. Both technologies integrates seamlessly with with Ethernet TSN leading to the emergence of Hybrid TSN architectures.

Within the TSN framework, time synchronization plays a key role in ensuring the proper operation of the network, particularly when traffic shaping and scheduling are involved. In TSN, the timeliness of data is ensured by precise synchronization of the clocks of devices in the network. This synchronization enables the separation of best-effort and realtime traffic, while also preventing contention for the transmission medium. It is evident that in a hybrid TSN network, the seamless propagation of time synchronization across different network segments and domains is crucial for the correct operation of the network.

In this context, the IEEE 1588 Precision Time Protocol (PTP) is the most widely used protocol for time synchronization in TSN networks. PTP is a distributed protocol that allows devices to synchronize their clocks with sub-microsecond accuracy. Focusing on wireless protocols, ensuring accurate time synchronization is particularly challenging due to the inherent characteristics of wireless communication, such as variable propagation delays, interference, and packet loss [4].

In this paper we focus on the assessment of the synchronization accuracy of IEEE 1588 (PTP) over 5G New Radio (NR) networks. We consider a scenario where a 5G NR network is used to interconnect TSN domains. Differently from [5]–[7], we evaluate the synchronization accuracy of PTP over 5G NR by considering different network configurations and traffic loads. The objective is to provide preliminary insights into the performance of PTP over 5G NR and its suitability for TSN applications.

The remainder of the paper is organized as follows. Section II provides an overview of the 5G NR TSN network architecture, the simulation setup and parameters. Section III presents the results of the simulation. Section IV concludes the paper.

II. Simulation Setup

A. 5G NR Network Architecture

To measure the synchronization accuracy of PTP over 5G, we implemented a simulation model using the ns-3 LENA–5G network simulator. The model, depicted in Fig. 1, consists of a 5G NR network that interconnects two TSN domains. Specifically, it includes a remote host, which is part of a local stationary TSN domain, and a 5G NR network that connects the remote host with a mobile TSN domain. The 5G NR network comprises a 5G base station (gNB) and two 5G user equipments (UEs). The Packet Data Network Gateway (PGW) links the two domains. It is important to note that we do not include in this simulation setup the implementation or models

This work has been partially funded by the EU Horizon Europe SNS JU PREDICT-6G (GA 101095890) Project. This manuscript reflects only the Authors' views and opinions, the EC can not be considered responsible for them.

TABLE I: Parameters used for the simulations.

Parameter	Value
Tx Power	35 dBm
Resource allocation algorithm	TDMA Round Robin
Beamforming	Ideal
Channel model	Urban Micro (UMi) street canyon
Channel shadowing	Disabled
Adaptive Modulation and Coding (AMC)	Enabled (error model)

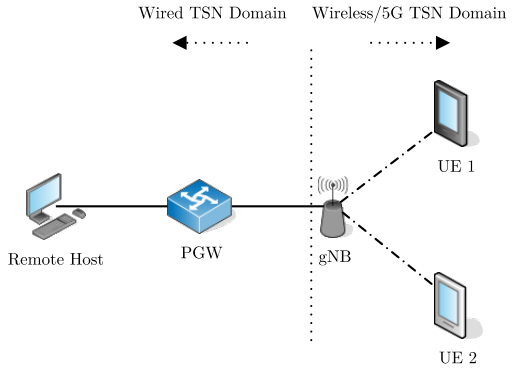

Fig. 1: 5G NR TSN network architecture.

of TSN mechanisms (e.g., traffic schedulers, shapers) nor 5G-specific functions such as TSN translators to interconnect the two TSN domains.

The gNB and the UEs operate in the mmWave frequency band. As shown in Fig. 2, the simulation setup utilizes two bands at 28 GHz and 28.2 GHz, each with a bandwidth of 50 MHz. Each band contains a single Component Carrier (CC), which in turn includes a single Bandwidth Part (BWP).

Both BWPs operate in Time Division Duplex (TDD) mode, with evenly distributed uplink and downlink slots. The NR standard defines numerologies $\mu = 0, 1, \ldots, 4$, where $\mu = 0$, the interface is compatible with Long-Term Evolution (LTE). Increasing the numerology decreases the symbol time and increases bandwidth usage, resulting in faster transmissions and lower latency due to more frequent scheduling. In this simulation setup, we use two different numerologies for the BWPs: $\mu = 4$ for BWP 1 and $\mu = 2$ for BWP 2. Each configured band is exclusively allocated to a specific UE, meaning that all uplink and downlink transmissions of UE1 occur on BWP1, while all transmissions of UE2 occur on BWP2.

Other relevant simulation parameters are reported in Table I.

B. Device model

We assume that each UE has its own local clock that can run independently from the other UEs and at a different rate with respect to the global simulator time. We additionally assume that the devices don't have any hardware timestamping capabilities, and the PTP messages are timestamped at the application layer. This clearly represents the worst case scenario, since software timestamping at the application level

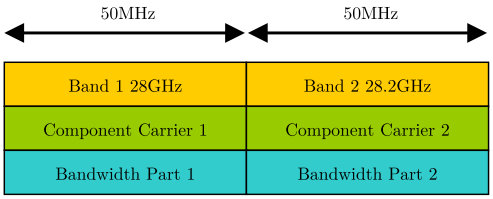

Fig. 2: Band allocation in the 5G NR network.

comprises delays introduced by the protocol stack and jitter due to concurrent running applications or uncertainties in the time acquisition. To include these aspects in the simulation, we model the timestamping and elaboration process as a random variable with a normal distribution with mean $\mu = 7300ns$ and standard deviation $\sigma = 580ns$ [8].

C. Clock model

We assume the Remote Host as the grand master of the PTP network, while the UEs as slaves. In particular, we assume the grand master has a high-precision clock C_m which correspond to the global simulator time C_g. So it yield that $C_m = C_g$. On the other hand, we suppose that the UEs have their own clock that can run at a different rate with respect to the global simulator time C_g. In particular, we opted to model the clocks C_s of the UEs with the relative clock model [9]. In particular,

$$C_s = \alpha C_m + \beta \tag{1}$$

where α is the relative clock frequency skew and β is the relative time offset or the initial difference between master and slave clocks. In this simulation setup, we set $\beta = 1ms$ for both UEs, while we set $\alpha = 1.001$ for UE1 and $\alpha = 0.999$ for UE2. This means that we expect a drift of $+1ms$ per second on the clock of UE1 while a drift of $-1ms$ per second on the clock of UE2.

D. Synchronization model

The synchronization model is based on the IEEE 1588 standard. Specifically, we implemented the Precision Time Protocol (PTP) using the end-to-end delay mechanism. Since Layer 2 (L2) transport is not compatible with the 5G NR network, we opted for UDP transport. PTP packets are encapsulated in UDP unicast packets and transmitted over the 5G NR network to their respective destinations. As previously mentioned, the Remote Host acts as the grandmaster clock, while the UEs function as slave clocks. Specifically, they are considered the Master Ordinary Clock (M-OC) and Slave Ordinary Clock (S-OC), respectively.

It is important to note that the network does not include any boundary clocks or transparent clocks; hence, the PGW and the gNB are not PTP-aware. They simply forward the PTP UDP-encapsulated datagrams as normal UDP datagrams without updating the PTP messages. In this simulation setup, the PTP update interval is set to one second. Each PTP transaction is allocated for transmission on the corresponding BWP for the specific UE.

TABLE II: Statistics of the estimated offset $\tilde{\Theta}$ by PTP.

Slave	Interf. (pps)	Mean (ns)	Std (ns)	Min (ns)	Max (ns)
1	0	1000028	1461	996836	1005080
	1000	1000053	1461	996819	1005065
2	0	-999966	1473	-1006062	-997840
	1000	-999992	1517	-1004064	-996895

E. Interfering traffic

To provide a more realistic scenario, we introduced interfering traffic in the network. Specifically, we considered a constant bit rate (CBR) traffic flow that generates UDP packets at a fixed rate. The interfering traffic is generated by the Remote Host, creating two flows, one for each UE. The interfering frames have a fixed length of 1500 bytes, and we examined two different scenarios in which they are sent at rates of 0 (i.e. no interfering traffic) and 1000 packets per second (pps). Similar to the PTP traffic, the interfering traffic is allocated on the corresponding BWP for each specific UE. It is important to note that no traffic-level prioritization features are utilized in this setup.

III. Results

In order to obtain a meaningful evaluation of the synchronization accuracy, we adopted a Monte-Carlo approach, repeating the experiments 5 times for each scenario, each with a different random number generator seed.

Let Θ be the real offset between the master and the slave clock, and let $\tilde{\Theta}$ be the offset estimated by PTP. Let define $\tilde{C_s} = C_s - \tilde{\Theta}$ as the slave time after PTP synchronization. It is then possible to define the synchronization error as $\Delta = C_m - \tilde{C_s}$. Remarkably, we refer to the synchronization offset as the difference between the master clock C_m and the slave clock C_s estimated by PTP, while the synchronization error Δ is the residual offset after synchronization, i.e., the difference between the master clock C_m and the slave clock $\tilde{C_s}$.

The first set of results concerns the synchronization offset $\tilde{\Theta}$ estimated by PTP. In particular, Figure 3 shows the trend of $\tilde{\Theta}$ at each synchronization step, while Table II reports the detailed statistics. As can be seen, the mean estimated offset is consistently close to the expected offset given by the relative clock model introduced in Section II-C, confirming the correct implementation and functionality of the PTP-based synchronization model. The numerology μ and the presence of interfering traffic do not lead to any substantial variation in the estimated offset, meaning the variability is mostly due to the intrinsic variabilities in the communication network and channel model, as well as to the timestamping inaccuracies and elaboration delays accounted for in the device model.

However, when examining the synchronization error Δ, some issues arise. In Fig. 4a and Fig. 4b, is reported the synchronization error Δ for $\mu = 4$ and $\mu = 2$, respectively. The statistics are detailed in Table III.

As can be seen, the residual offset remains significant across all simulated scenarios post-synchronization. It is important to note that PTP is designed with the assumption of symmetrical propagation delay. However, in this specific case, Table IV shows that the uplink (UL, i.e., from a UE to the remote host) and downlink (DL, i.e., from the remote host to the UE) propagation delays are not symmetrical. This asymmetry leads to a systemic error in the estimated offset $\tilde{\Theta}$, resulting in a constant offset between C_m and $\tilde{C_s}$.

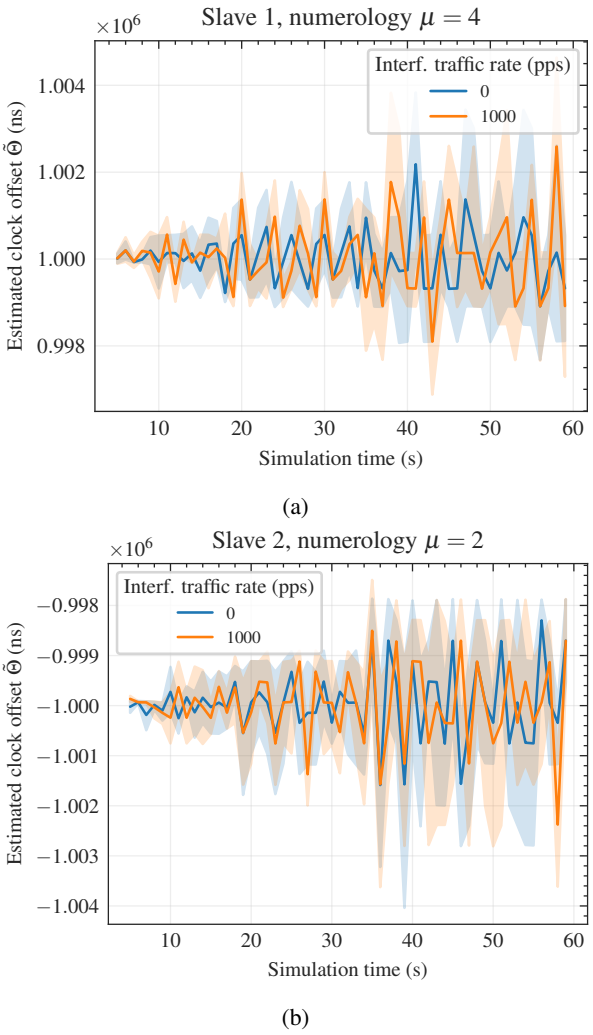

Fig. 3: Estimated offset $\tilde{\Theta}$ by PTP. (a) $\mu = 4$ (b) $\mu = 2$.

Unlike the estimated offset, the synchronization error Δ is influenced by the numerology μ and the presence of interfering traffic. Higher numerologies lead to a lower residual offset, as shown in Table IV, where $\mu = 4$ results in a significant reduction in both DL and UL latencies. It appears that higher numerologies attenuate asymmetries, thereby reducing Δ.

Regarding interfering traffic, the results follow a counter-intuitive trend. Regardless of the numerology considered, the synchronization error is lower in the presence of interfering traffic. It seems that interfering traffic affects the DL latency more significantly, while UL latency is influenced by other factors. As in the previous case, the increase in DL latency reduces asymmetry, leading to a lower synchronization error.

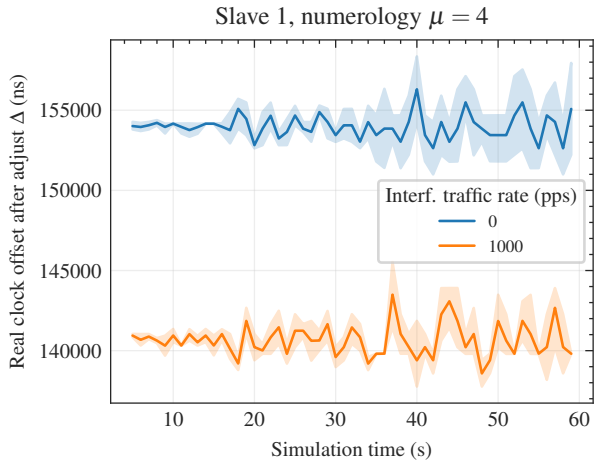

(a)

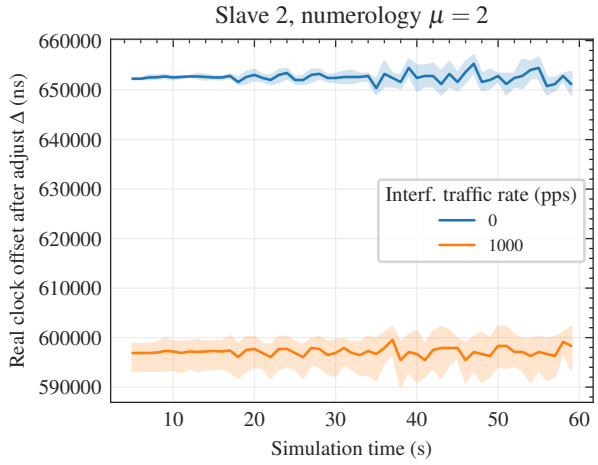

(b)

Fig. 4: Synchronization error Δ, i.e. residual offset, after PTP synchronization. (a) $\mu = 4$ (b) $\mu = 2$.

TABLE III: Statistics of the residual synchronization offset Δ by PTP.

Slave	Interf. (pps)	Mean (ns)	Std (ns)	Min (ns)	Max (ns)
1	0	153987	1711	150550	158788
	1000	140664	1546	137753	145961
2	0	652573	1829	649149	657386
	1000	597139	4134	586663	603810

We want to emphasize that the results presented in this section are preliminary, and further analysis is needed to better understand the impact of numerology and interfering traffic on the synchronization accuracy of PTP. This will help to provide and test an optimized configuration for the 5G NR network.

IV. Conclusions

In this paper, we provided a preliminary assessment of the synchronization accuracy of PTP over mmWave 5G NR networks. We implemented a simulation model using the ns-3 network simulator, incorporating models of the 5G NR network architecture, devices, clocks, and synchronization processes. We evaluated the synchronization accuracy of PTP over 5G NR under various network configurations and traffic loads. The results indicated that the synchronization accuracy of PTP over 5G NR is influenced by numerology and the presence of interfering traffic, with systemic residual offsets potentially arising from asymmetries in propagation delays. Future work will focus on further improving the simulation model and testing different configurations and parameters, such as using Frequency Division Duplexing (FDD), to mitigate inaccuracies caused by asymmetrical delays.

TABLE IV: Statistics of the PTP traffic latency.

Slave	Interf. (pps)	Traffic direction	Mean (μs)	Jitter (μs)
1	0	DL	285	31
		UL	615	8
	1000	DL	313	59
		UL	626	8
2	0	DL	855	60
		UL	2243	28
	1000	DL	907	59
		UL	2160	26

References

[1] S. Sudhakaran, V. Mageshkumar, A. Baxi, and D. Cavalcanti, "Enabling QoS for Collaborative Robotics Applications with Wireless TSN," in *2021 IEEE International Conference on Communications Workshops (ICC Workshops)*, (Montreal, QC, Canada), pp. 1–6, IEEE, June 2021.

[2] S. Sudhakaran, K. Montgomery, M. Kashef, D. Cavalcanti, and R. Candell, "Wireless Time Sensitive Networking Impact on an Industrial Collaborative Robotic Workcell," *IEEE Transactions on Industrial Informatics*, vol. 18, pp. 7351–7360, Oct. 2022.

[3] A. Morato, G. Frigo, and F. Tramarin, "Optimized 5G Communication Infrastructure for PMU-Based Distributed Measurement Systems," in *2023 IEEE 13th International Workshop on Applied Measurements for Power Systems (AMPS)*, pp. 01–06, Sept. 2023.

[4] S. Sudhakaran, C. Hall, D. Cavalcanti, A. Morato, C. Zunino, and F. Tramarin, "Measurement method for end-to-end Time synchronization of wired and wireless TSN," in *2023 IEEE International Instrumentation and Measurement Technology Conference (I2MTC)*, (Kuala Lumpur, Malaysia), pp. 1–6, IEEE, May 2023.

[5] M. Gundall, C. Huber, P. Rost, R. Halfmann, and H. D. Schotten, "Integration of 5G with TSN as Prerequisite for a Highly Flexible Future Industrial Automation: Time Synchronization based on IEEE 802.1AS," in *IECON 2020 The 46th Annual Conference of the IEEE Industrial Electronics Society*, pp. 3823–3830, Oct. 2020.

[6] D. Patel, J. Diachina, S. Ruffini, M. De Andrade, J. Sachs, and D. P. Venmani, "Time error analysis of 5G time synchronization solutions for time aware industrial networks," in *2021 IEEE International Symposium on Precision Clock Synchronization for Measurement, Control, and Communication (ISPCS)*, pp. 1–6, Oct. 2021.

[7] M.-T. Thi, S. Guédon, S. B. H. Said, M. Boc, D. Miras, J.-B. Dore, M. Laugeois, X. Popon, and B. Miscopein, "IEEE 802.1 TSN Time Synchronization over Wi-Fi and 5G Mobile Networks," in *2022 IEEE 96th Vehicular Technology Conference (VTC2022-Fall)*, pp. 1–7, Sept. 2022.

[8] A. Mahmood, R. Exel, and T. Sauter, "Delay and Jitter Characterization for Software-Based Clock Synchronization Over WLAN Using PTP," *IEEE Transactions on Industrial Informatics*, vol. 10, pp. 1198–1206, May 2014.

[9] G. Giorgi and C. Narduzzi, "Modeling and Simulation Analysis of PTP Clock Servo," in *Control and Communication 2007 IEEE International Symposium on Precision Clock Synchronization for Measurement*, pp. 155–161, Oct. 2007.